4.2 AN AIRCRAFT FLIGHT THROUGH A REAR-FLANK DOWNDRAFT: REVISITING AN OLD CASE

Donald W. Burgess *
Cooperative Institute for Mesoscale Meteorological Studies, University of Oklahoma/NSSL, Norman, OK

1. INTRODUCTION

Rear-flank downdrafts (RFDs) associated with hook echoes of supercell thunderstorms have been observed for over 50 years (see the discussion in Markowski 2002; hereafter M02). The potential importance of the RFD in tornadogenesis has been hypothesized for nearly as long (again, see the discussion in M02). Particularly, since the advent of research with coherent radars (1970's), the association between the RFD, the formation of the low-level mesocyclone, and later tornadogenesis has been shown to be quite strong.

A significant number of the research cases that emphasized the relationship between the RFD and tornadogenesis arose from the Verification of the Origins of Rotation in Tornadoes Experiment, Field Phase 1 (VORTEX1). Direct surface observations of RFDs within tornadic and non-tornadic supercells were a prominent VORTEX1 contribution (Markowski et al. 2002; hereafter ME02). Unfortunately, VORTEX1 was not able to observe RFD characteristics above the surface, and very few direct observations of RFDs aloft have ever been made (M02). Observations of RFDs aloft have not resulted from smaller-scale supercell field programs that have occurred in the years following VORTEX1.

Interestingly, one of the early NSSL Dual-Doppler cases, one of those that was used to help determine the association between the RFD and tornadogenesis, 8 June 1974, contains an aircraft flight through an RFD. For reasons that this author will not pursue in this paper, those RFD-aloft observations have never been presented although the analysis was done some 32 years ago.

This paper will summarize the 8 June 1974 storm (Section 2), give information on data sources used in the analysis (Section 3), discuss the results of the analysis (Section 4), and offer a few concluding comments (Sections 5).

* *corresponding author address:* Don Burgess, NSSL/WRDD/Rm. 3933, National Weather Center, 120 David L. Boren Blvd, Norman, OK 73072-7323; e-mail: Donald.Burgess@noaa.gov

2. 8 JUNE 1974 SUPERCELL

The 8 June 1974 case was studied by several groups (Ray 1976, Ray et al. 1976, Brandes 1977, Burgess et al. 1977, Eagleman and Lin 1977, Brandes 1978, and, perhaps, others). The studies focused on single and Dual-Doppler data collection on a tornadic supercell that began southwest of Oklahoma City, moved across the city, and continued well northeast of the city (Fig 1) and a later storm (the Harrah storm) not discussed in this paper. The 1974 Oklahoma City storm (not to be confused with multiple Oklahoma City storms in earlier years or later years) formed ahead of an advancing dryline just after noon and was the first of a number of tornadic supercells that made up a substantial regional tornado outbreak.

The Oklahoma City storm produced 3 tornadoes with the first and third tornadoes occurring near the low-level center of circulation and the second tornado occurring along the storm gust front south of the center of circulation. An NSSL damage survey was performed. The sense of rotation for all three tornadoes was cyclonic. The first tornado began with damage at the NWS Office on the southwest side of the city at 1342 (all times are CST) and continued for 10 km to near city center (~1354). Tornado 1 produced mostly lesser (F0/F1) damage along its swath, but did produce a few areas of moderate (F2/F3) damage. Tornado 2 (Spencer tornado) began about 1406 at the northeast edge of Spencer and continued for 6 km (until ~1412). Spencer tornado damage was F0/F1 everywhere along the path except at one location where a mobile home was destroyed and vehicles were overturned (F2 damage was determined by NWS surveyors). Tornado 3 (Luther tornado) began about 1412 between Spencer and Luther, and traveled for 17 km before dissipating just south of Luther (~1430). The Luther tornado was stronger, considerably wider, and tracked for a longer distance than the first two tornadoes. Although it traversed mostly rural areas, it completely destroyed two houses and downed several large high-voltage transmission towers; damage easily justifying an F3 rating. No other tornadoes were reported from the storm, but storm B (shown in Fig 1) that formed on the right flank of the Oklahoma City Storm went on to produce devastating (F4) tornadoes at Drumright and in the Tulsa area.

3. DATA SOURCES

This paper relies on data from radar and aircraft. Doppler radar measurements used here are from the analysis done by Burgess et al 1977 (hereafter BE77). They used NSSL Doppler radars at NSSL (Norman) and Cimarron Airport (location shown in Fig 1). Both radars were 10-cm, had 0.8 deg beam width, had 600 m gate spacing, and used PRFs corresponding to a Nyquist velocity interval of +/- 35 m/s. Radar volume scan times were slow by current standards, taking nearly 10 minutes to complete one volume. Details on the steps and procedures for dual-Doppler computation are in BE77. Horizontal and vertical grid spacing was 1 km. Horizontal wind vectors are displayed with the individual-level mean wind vector removed. Various error sources limited the accuracy of vertical velocity estimates. Although several dual-Doppler and single-Doppler analyses are mentioned in BE77, only one analysis time (1409) is used here.

Aircraft data were from the University of Wyoming Queen Air. Some information about Queen Air research objectives, control and coordination, and operation times are in the NSSL 1974 Spring Summary (edited by Barnes 1974). Funding for use of the aircraft was provided by a National Science Foundation Grant. John McCarthy, University of Oklahoma, was PI on the grant. For the June 8 flights, Don Veal likely was the aircraft pilot, but exact information on personnel for that flight no longer exists. Aircraft measurements included pressure, altitude, temperature, dew-point temperature, equivalent potential temperature (Theta-e), wet-bulb potential temperature (Theta-w; data not shown) and rate of climb. Aircraft heading, wind direction, and wind speed were also recorded, but accurate direction and speed estimates required a continuous period of straight and level flight which did not occur for the analyzed flight leg. The raw data had sample rates of multiple times per second. These were averaged to produce 1 second data. Finally, a weighted, 3-point filter was passed over the data to remove additional noisiness. Neither the original nor the averaged/filtered data have been preserved. A transcription of the aircraft voice recorder (push-to-talk for selected events) is available to help interpret the aircraft data.

The aircraft took off from Max Westheimer airport (OUN) in Norman at 1156, just as developing cumulus congestus cloud towers along the dry line were making their first radar echoes. The aircraft mission was to obtain data on growing cumulus clouds, obtain data near updraft areas of mature thunderstorms, and release chaff in clear-air areas near the storm to extend the area of useable Doppler radar data. The aircraft performed many flight segments/legs during 2 flights: 1156-1450 and 1530-1730. The flight segment analyzed here began at 1354 and lasted until 1417. During that time the aircraft flew around the back of the storm (from left to right rear), descending from 4100 m to 700 m (all heights are AGL). After descent, the aircraft flew along the right flank of the storm in the outflow region, in the inflow region, and back into the outflow region before moving off the south to investigate developing storm B.

Data on vertical atmospheric structure and evolution were available from 7 rawinsonde releases at OUN and 5 rawindsonde releases at FSI during the morning to evening period. The OUN release at 1115 was judged the best pre-storm sounding for the Oklahoma City storm. Also available were vertical profiles from Queen Air climb-outs, in-flight ascents and descents, and landings.

Pictures of cloud formations at certain points in the flights (but not the tornadoes) were available from a hand-held camera in the cockpit. Pictures of cloud formations and all three tornadoes were available from NSSL and OU intercept teams and from pictures collected from the general public.

4. Results

A portion of the Queen Air flight path is shown (Fig 2) overlaid on the 1409 dual-Doppler analysis at 1.3 km height. The aircraft track has been time-to-space converted to the 1409 Doppler analysis time. From traces of selected aircraft data (Fig 3), it can be seen that the Queen Air was at 850 mb (~1.1 km) at 1406, completing its descent around the back of the storm. The aircraft voice recording transcript indicates that the pilot planned to level the plane at 880 mb (0.7 km; near ambient cloud base height) and fly the low-level part of the track at constant altitude. The pilot was still in the leveling process when the plane first encountered the RFD (~1408:30). After traversing the RFD and rear gust front (~1409:45), the plane flew into the inflow and began releasing packets of chaff. [Note that the chaff releases did not occur in time to affect the radar echo area at 1409 although the chaff may have provided slightly more echo area at the 1420 analysis time (not shown). In general, the strong inflow winds blew the chaff into the existing precipitation echo too quickly for much additional echo area to be realized.] It is clear from the voice transcript that the pilot saw the Spencer tornado (T in Fig 2) along the gust front and kept somewhat constant distance from it for a few minutes. A picture of the Spencer tornado (Fig 4) illustrates what the pilot saw. About 1412, the more dramatic Luther tornado formed (at relative location

C in Fig 2), and it too was seen by the pilot. A view of the Luther tornado during its mature stage (~1418) is Fig 5. Perhaps, because of the Luther tornado or because of an already planned flight path, the aircraft circled back to the southwest (between the Luther tornado and where the Spencer tornado had just dissipated), penetrating the rear gust front and encountering cold outflow (~1412:20). At a relative position just outside the low-level radar echo, the aircraft again encountered the RFD (~1414).

It should be mentioned that gust front/air mass boundaries shown in Fig 3 and discussed in the previous paragraph are subjective estimates. However, they are based on integrated interpretation of all the aircraft data. In particular, both RFD encounters have similar Theta-e drops produced by temperature increases and dew point/Theta-w decreases (data not shown in Fig 3). The first gust front penetration is marked by a relative maximum in rate of climb (ROC) and a return to temperature (T) and Theta-e associated with parts of the track within inflow/undisturbed boundary-layer air. The second gust front penetration is marked by a strong maximum in ROC (1500 ft/min; implied updraft of 7.6 m/sec) and a drop of more than 2 deg in T. The traverse through the air behind the gust front on the second penetration is of interest. T is more than 2 deg colder than the inflow, but Theta-e values are unchanged from the inflow. Its properties suggest that it might be boundary-layer air cooled through a "wet-bulb" effect within precipitation. The origin of this air mass is unknown, but it could be inflow/boundary-layer air that ascended over the forward flank gust front, descended in the forward-flank downdraft, and was cooled by precipitation as it circled around the low-level mesocyclone.

It is interesting to speculate on the vertical velocity of the RFD and the origin of the air sampled within it. Unfortunately, both penetrations of the RFD occurred as the pilot was applying power to recover the aircraft to level flight (~880 mb). The first RFD penetration appeared to occur after the pilot overshot the 880 mb level on descent. The second RFD penetration occurred while the pilot was trying to recover from the sharp rise associated with updraft along the rear gust front. Dual-Doppler velocity estimates at 1409 (Fig 2) indicate downdraft near the portion of the aircraft track behind the rear gust front and within precipitation (just before 1414), but, qualitatively, only weak downward motions are suggested.

Information about RFD structure can be obtained from comparing the aircraft-observed values of RFD Theta-e to Theta-e values in the storm's environment. Vertical profiles of Theta-a from the 1115 Norman sounding and from the 1354-1408 descent of the Queen Air (Fig 6) are similar and give some confidence that the profiles can be trusted. The minimum Theta-e value from the RFD penetrations (~349 K) is found to be within the sharp drop in Theta-e that occurred just above the top of the boundary layer. The supposed magnitude of the descent of air parcels would be ~70 mb (~700 m). However, as pointed out by ME02, care must be taken when trying to use Theta-e to estimate the origin of air parcels. Complete Theta-e conservation for parcels (no entrainment) is unlikely. ME02 conclude their discussion about parcel origin by saying "It perhaps is most appropriate to denote [the height of parcel origin] as simply the height on an inflow sounding where Theta-e values are equal to those observed…within the downdraft, rather than as a measure of parcel origin." The same will apply to use of Theta-e in this paper. However, in this case, the minimum Theta-e was associated with reduction in Theta-w, suggesting that at least some of the air came from the upper, dry side of the inversion separating the moister boundary layer from dry air above.

5. CONCLUDING REMARKS

It is interesting, and perhaps a little sad, to note that the best observational data on thermodynamics of RFDs above the surface may have come from a data set that was collected 34 years ago. That said, there is really nothing startling about these above-the-surface data. The location and magnitudes of quantities within the RFD are in general agreement with subsequent radar and surface RFD data collected since 1974. The conceptual model associated with the June 8 case fits the ME002 model (surface model; their Fig 14) where low Theta-e deficits surround tornado locations for Significant Tornadic Supercells, with larger deficits (if any) occurring further to the west and south of the tornado. In the June 8 case, there was no Theta-e deficit for the portion of the path that was closest to the significant Luther tornado. Indeed, in this paper the area closer to the tornado is not even necessarily identified as RFD. South of the hook, further from the tornado and in what here was called RFD, there was a Theta-e deficit of up to 7 deg K, a little more than the 5 deg K threshold established by ME02, but at a location far enough away from the significant tornado to be permitted by the model.

Of course, for the June 8 case, no surface Theta-e data were collected, nor was there the collection of high time-and-space-resolution Doppler data. That is, a complete data set from which the full character of the RFD could be determined was not collected. The overarching objective of the upcoming VORTEX2 project (VORTEX2 Steering Committee 2008) is to collect complete data sets that will answer questions about tornadogenesis and the role that RFDs might play. Hopefully, using UAS (Unmanned Aeronautical Systems; UAVs and associated infrastructure to support them) much more and better RFD data can be collected above the surface and combined with other VORTEX2 instruments (e.g. mobile radars, mobile mesonets and other surface probes, and sounding vehicles) to gain greater understanding of RFDs. Of particular utility might be mobile Doppler radars with dual-polarization capability (see Romine et al. 2008 for discussion of potential importance of dual-polarization information in understanding tornadic supercells).

6. ACKNOWLEDGMENTS

I am indebted to my co-authors on the 1977 paper (Rodger Brown, Les Lemon, and Chuck Staffford) who greatly contributed to analyses that made it possible to go back and add analysis of aircraft data to the case at this late date. I especially thank Rodger for recent help in unearthing documentation for the 1974 Spring Program and for reviewing the paper. I am grateful to John McCarthy for sharing the Queen Air data those many years ago. I am also grateful to those who flew and maintained the aircraft and to those who helped with Doppler data collection and other parts of the 1974 Spring Program.

7. REFERENCES

Barnes, S.L., Editor, 1974: Summary of the 1974 Severe Thunderstorm Observation Season and Operations. Special Report, DOC/ERL/NSSL, 145 pgs. [Available from the author.]

Brandes, E.A., 1977: Gust front evolution and tornado genesis as viewed from Doppler radar. *J. of Applied Met.*, **16**, 333-338.

_____, 1978: Mesocyclone evolution and tornadogenesis: Some observations. *Mo.n Wea. Rev.*, **106**, 995-1011.

Burgess, D.W., R.A. Brown, L.R. Lemon, and C.R. Stafford, 1977: Evolution of a tornadic thunderstorm. Preprints, *10th Conf. on Severe Local Storms*, AMS, Omaha, NE, 84-89.

Eagleman, J.R., and W.C. Lin, 1977: Severe thunderstorm internal structure from dual-Doppler radar measurements. *J. of Applied Met.*, **16**, 1036-1048.

Markowski, P.M., 2002: Hook echoes and rear-lfank downdrafts: a review. *Mon. Wea. Rev.*, **130,** 852-876.

_____, J.M. Straka, and E.M. Rasmussen, 2002: Direct surface thermodynamic observations within rear-flank downdrafts. *Mon.Wea. Rev.*, **130**, 1692-1721.

Ray, P.S., 1976: Vorticity and divergence fields within tornadic storms from Dual-Doppler Observations. *J. of Applied Met.*, **15**, 879-890.

_____, C.E. Hane, R.P. Davies-Jones, and R.A. Alberty, 1976: Tornado-parent storm relationship deduced from a dual-Doppler radar analysis. *Geo. Res. Letters*, **3,** 721-723.

Romine, G.S., D.W. Burgess, and R.B. Wilhelmson, 2008: A dual-polarization-radar-based assessment of the 8 May 2003 Oklahoma City area tornadic supercell. *Mon.Wea. Rev.*, **136**, 2849-2870.

VORTEX2 Steering Committee, 2008: Documents contained at http://www.vortex2.org/

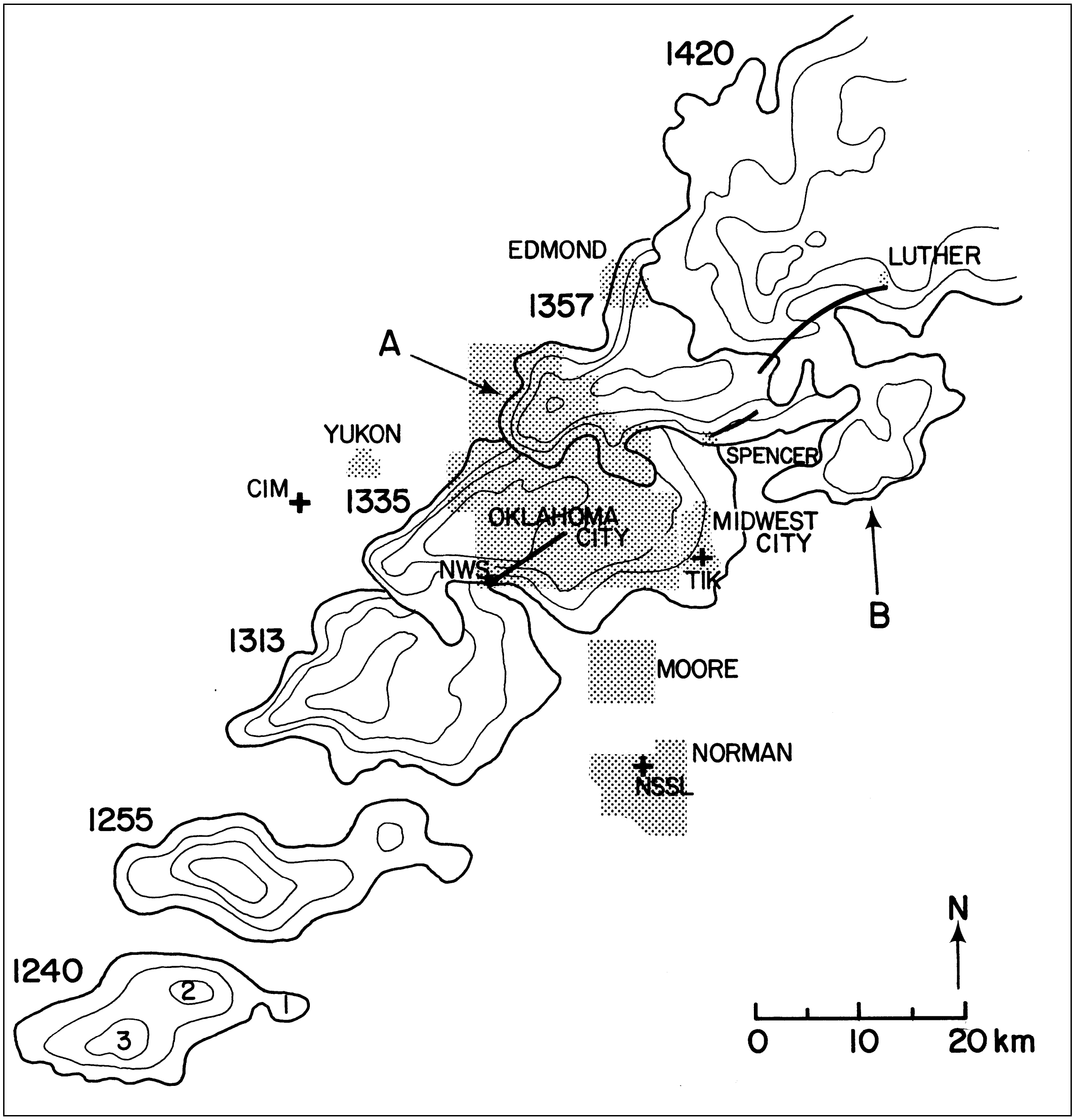

Figure 1. Track of the Oklahoma City storm of 8 June 1974. Low-level Doppler reflectivity fields at selected times (CST) are contoured in 10 dBZ intervals, beginning with 20 dBZ. Stippling indicates population centers; Cimarron Doppler is CIM. Flanking storms A and B are marked. Tornado damage tracks from NSSL survey are indicated by thick, dark lines.

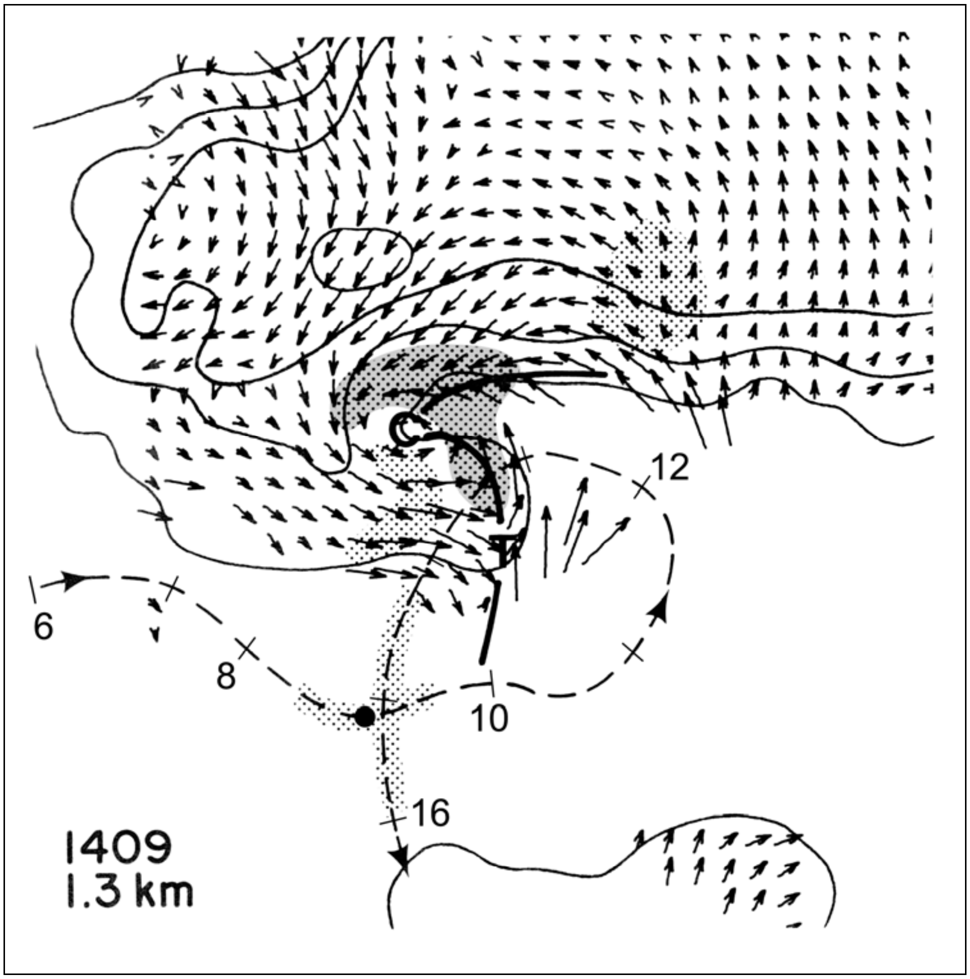

Figure 2. Dual-Doppler analysis at 1409 CST at 1.3 km AGL. Reflectivity contours are at 10 dBZ intervals, beginning at 20 dBZ. Wind vectors are relative to the 1.3 km mean vector for the full analysis area (larger than the figure area). Dark shading indicates updraft (~5 m/s and greater), light shading within 20 dBZ contour indicates downdraft (~2.5 m/s and greater). Dashed line is Wyoming Queen Air flight track with time in minutes after 1400 CST annotated. Aircraft location at 1409 CST is dark circle. Light shading outside of 20 dBZ echo is estimated downdraft location from aircraft data. Dark solid lines are estimated locations of rear and forward flank gust fronts. Spencer tornado location (T) and circulation center (C; relative location of later development of Luther tornado) are marked.

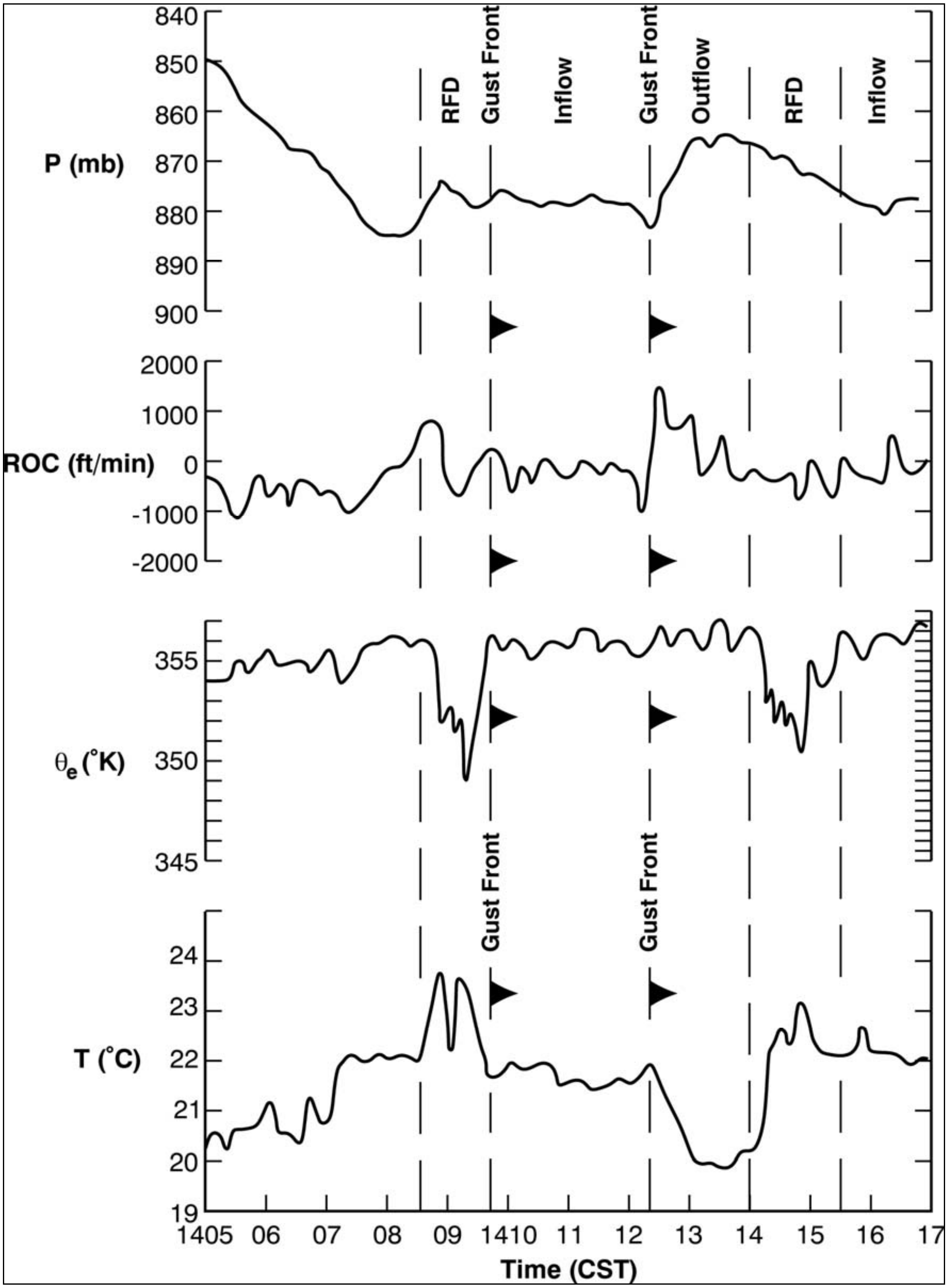

Figure 3. Plots of selected Wyoming Queen Air aircraft parameters for a segment of a flight on June 8, 1974. Pressure (P), Rate of Climb (ROC), Theta-e, and Temperature (T) are plotted. Vertical dashed lines are subjective estimates of air mass boundaries; RFD is Rear-Flank Downdraft.

Figure 4. Spencer tornado at ~1408 CST, looking east from a rural location northeast of Spencer. Photograph was taken by a member of the general public whose name, unfortunately, has been lost.

Figure 5. Luther tornado at ~1418 CST, looking northwest from a location northeast of Spencer and southwest of Luther, and about equal distance between towns. Photograph courtesy of H. E. McClain.

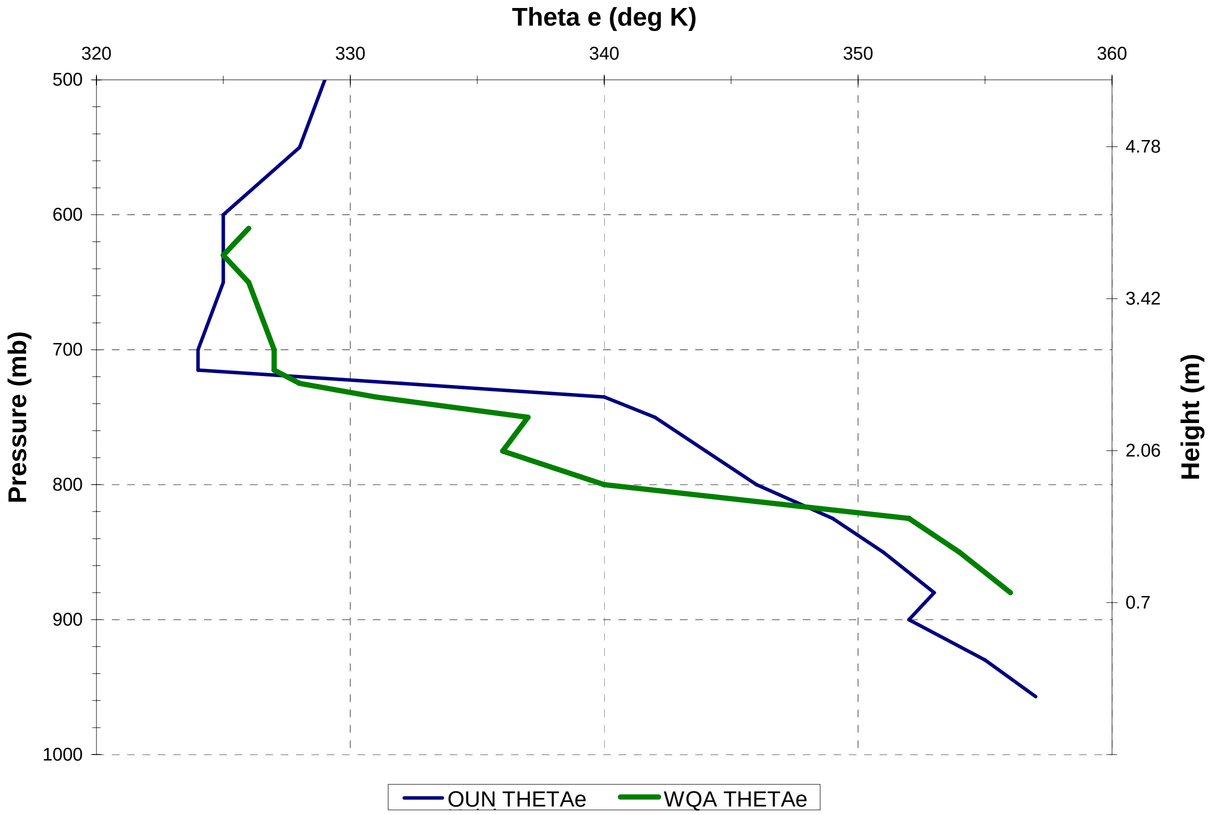

Figure 6. Plot of Theta-e from the 1115 CST Norman (OUN) sounding and the Wyoming Queen Air aircraft (WQA) descent (1354 - 1408 CST).